

# Phosphorylated poly(vinyl alcohol) surface coatings as intumescent flame inhibitor for polymer matrix composites

Stefano Scurti, Jacopo Ortolani<sup>\*</sup>, Alberto Ghirri, Emanuele Maccaferri<sup>\*</sup>, Daniele Caretti, Laura Mazzocchetti

Department of Industrial Chemistry "Toso Montanari", University of Bologna, Viale Risorgimento 4, 40136 Bologna, Italy

## ARTICLE INFO

### Keywords:

PPVA  
Intumescent coating  
Flame inhibitor  
CFRP  
Phosphorous  
Cone-calorimeter

## ABSTRACT

Flammability is one of the main drawbacks affecting polymer matrix composites (PMCs), limiting metal replacement in several applications. Phosphorus compounds demonstrated a great ability in contrasting fire spreading. Here, phosphorylated poly(vinyl alcohol) (PPVA) has been synthesized and used as an intumescent flame inhibitor coating for carbon fiber reinforced polymer (CFRP) laminates. The synthesized PPVAs, with a phosphorylation degree up to 7.5 %wt, were investigated by spectroscopic (NMR and IR) and thermal (TGA and DSC) analyses. Moreover, thermal degradation kinetics was also rationalized by applying differential and integrals methods: the phosphorus catalytic effect combined with radicals-coupling behaviour deriving from the phosphorus species developed during the combustion has been highlighted, confirming the inhibitor role of PPVAs. Cone-calorimeter tests, simulating a small-scale fire scenario, were carried out on poly(vinyl alcohol)-coated and PPVA-coated materials prepared by solvent casting. Results highlight the anti-flame properties of PPVAs, especially as effective flame inhibitors: up to -58 % in the time of flame (TOF). Instead, poly(vinyl alcohol) coatings lead to an overall worsening of the material fire behaviour, highlighting the crucial role of phosphorous to reduce flammability. Such promising results pave the way for the use of PPVA coatings to reduce the fire risk of flammable composites making them safer.

## 1. Introduction

In the last two decades, the use of polymer matrix composites (PMCs) in structural applications experienced rapid growth thanks to their excellent mechanical properties and lightweight. In particular, carbon fiber reinforced polymers (CFRPs) with thermosetting matrices represent a viable alternative to replace metals due to their high specific stiffness and strength [1,2]. However, the organic nature of the matrix increases the risk of combustion, limiting the application of such composites in fields with a high fire hazard. The combustion, besides causing decay of mechanical properties until complete component structural failure, produces important emissions of heat, volatile organic compounds (VOCs) and smoke, representing a risk to human safety [3–6]. Therefore, trying to reduce the overall flammability of PMCs is of paramount importance. Several approaches can be addressed, such as adding flame retardant (FR) additives and coatings, even nanostructured [7–10]. Unfortunately, the addition of FRs directly into the matrix will impact the bulk of the material affecting mechanical properties and also

the resin crosslinking [11,12].

A series of FR additives, such as hydrates, silicates, carbonates, metal oxides, sulphides, and phosphorus compounds, have been developed [13–17]. Intumescent flame retardant agents based on phosphorus compounds are widely used due to their ability to form char by a condensed-phase mechanism that can insulate the underlying polymer from heat and oxygen. Moreover, the water vapour derived from the dehydration reaction can dilute flammable gases, thus quenching the flame [18,19]. Furthermore, the lower toxicity of these additives compared to halogen-based and aromatic-based systems represents a benefit for both human health and the environment [5]. In particular, organo-phosphorous polymers represent the most suitable systems to prevent, delay or inhibit the flame [20–22]. Several strategies have been developed to insert phosphoric, phosphonic and phosphinic acid moieties in the macromolecular side chain, such as functionalizing vinylic or allylic monomer with a group containing phosphorous, direct polymerization of specific monomers, as well as post-polymerization reactions [23,24]. Wang and co-workers developed ethylene-vinyl acetate

<sup>\*</sup> Corresponding authors.

E-mail addresses: [jacopo.ortolani3@unibo.it](mailto:jacopo.ortolani3@unibo.it) (J. Ortolani), [emanuele.maccaferri3@unibo.it](mailto:emanuele.maccaferri3@unibo.it) (E. Maccaferri).

<https://doi.org/10.1016/j.porgcoat.2023.107457>

Received 5 October 2022; Received in revised form 27 January 2023; Accepted 31 January 2023

Available online 8 February 2023

0300-9440/© 2023 Elsevier B.V. All rights reserved.

copolymers grafted with diphenyl chlorophosphite (DPCP) to enhance the thermal stability in high-density polyethylene blends, but the lack of miscibility of the pair leads to a decreased mechanical properties [21]. Shree et al., instead, succeeded in preparing an epoxy resin modified with phytic acid phosphorylated hyperbranched polyols as a transparent intumescent coating [25]. The same approach was investigated by Yan's group that, via a multi-step route, synthesized flexible phosphate esters applied into amino resin to obtain an intumescent coating for plywood boards [26]. In a different attempt, an in situ photopolymerization of vinyl-phosphonic acid with a cyanurate in presence of crosslinking agents was carried out to coat glass fiber-reinforced epoxy resin (GRE) to improve their thermal stability by Williams and co-workers [27]. Since it has been recognized that combustion is primarily a surface-occurring process, the simultaneous effect derived from the phosphorous moieties with the surface application of the anti-flame additives, which would also prevent bulk properties modification, appears as a highly suitable approach [28]. Moreover, it allows to treat different types of substrates, such as wood, textiles, and plastics [29–32]. For these reasons, the employment of phosphorus-based polymeric FR films has been extensively reported in the literature. Despite the employment of phosphorous functionalized bio-degradable polymers, such as poly(vinyl alcohol) (PVA), represents a suitable and sustainable approach to realize hybrid inorganic-polymers [21,33], nanocomposite films [34,35], and grafted polymeric surface coatings [36,37], the reported products derive by a tedious and complex synthetic route. Moreover, optically transparent intumescent coatings applied to CRFPs are slightly investigated. CRFPs are often employed also in finishing components to impart a luxurious and high-end aspect, and the ability to protect the composite while simultaneously guaranteeing a pleasing aesthetic is extremely important.

In the present work, a phosphorylated poly(vinyl alcohol) (PPVA) is proposed as a flame-inhibitor coating for polymer matrix composite materials, using epoxy-based CFRP laminates as substrate. A novel and practical strategy has been proposed to control copolymers' composition and enhance the phosphorous content. Spectroscopic and thermal analyses were carried out to investigate the structure-properties correlation of the phosphorylated material. The PPVA's ability to form homogeneous films was exploited to apply it as a surface coating onto the composite substrate. The fire resistance of PPVA-coated CFRPs was evaluated by cone-calorimeter tests, simulating a small-scale fire scenario. The effect of both coating grammage and PPVA phosphorylation degree on the fire resistance behaviour was investigated, as well as the kinetic of PPVA thermal decomposition.

## 2. Experimental section

### 2.1. Materials

2,2'-Azo-bis-isobutyronitrile (AIBN), vinyl acetate (VA, >99 %), sodium hydroxide (NaOH), potassium phosphate ( $K_3PO_4$ ), potassium hydrogen phthalate ( $C_8H_5KO_4$ ), ortho-phosphoric acid ( $H_3PO_4$ , 98 %) and sodium chloride (NaCl) were purchased from Sigma Aldrich (Italy). The solvents (methanol, ethanol, acetone, ethyl ether) were used without further processes of purification. Composite specimens for cone-calorimeter tests are made of 2 plies of twill  $2 \times 2$  weave T700 carbon fabric in epoxy matrix prepregs (GG630T-DT121H), cured in an autoclave for 2 h at 135 °C, 6 bar external pressure. The resulting laminate thickness is  $(1.32 \pm 0.06)$  mm.

### 2.2. Synthesis of poly(vinyl acetate) (PVAc)

Following the experimental methodology described in a previous work [38], the polymerization reaction of vinyl acetate (VAc) was carried out in a three-necked flask placed under a nitrogen atmosphere. The PVAc was synthesized by dissolving 10 mL of VAc monomer (0.1 mol) in 10 mL of ethanol. After heating the solution up to 70 °C, the AIBN

initiator was added (0.1 % mol/mol with respect to VAc). The reaction was stirred for 90 min. Then, the mixture was cooled down to room temperature and poured in ethyl ether. The polymer was filtered and washed several times with ethyl ether. The PVAc was characterized by nuclear magnetic resonance (NMR), and Fourier-transform infrared (FT-IR) spectroscopy.

### 2.3. Synthesis of poly(vinyl alcohol) (PVA)

The direct saponification reaction of poly(vinyl acetate) was carried out in a 100 mL flask, in which 0.5 g of PVAc was added in 8 mL of acetone. The mixture was stirred at 50 °C to promote the solubilization of the polymer. Once dissolved, NaOH 1 M in methanol was added (1:1.5 mol/mol). The reaction mixture was kept for 1 h under reflux. Then, the mixture was filtered, and the methanol was evaporated. The fully hydrolysed polymer was dried in an oven at 70 °C for 2 h, according to a previous work [38]. The PVA was characterized by NMR, FT-IR spectroscopy, thermogravimetric analysis (TGA) and differential scanning calorimetry (DSC).

### 2.4. Synthesis of phosphorylated poly(vinyl alcohol) (PPVA)

The phosphorylated poly(vinyl alcohol) (PPVA) was obtained by a post-polymerization reaction. The copolymer was synthesized by dissolving  $H_3PO_4$  in 10 mL of distilled water; the amount of phosphoric acid was varied to obtain a solution ranging from 0.3 to 15 M in order to modulate the phosphorylation degree. After its complete dissolution in water, 1 g of PVA was added and the solution was refluxed for 100 min. In the end, the mixture was poured into acetone. The polymer was filtered and washed several times with acetone. The product obtained was dried in an oven at 60 °C to remove traces of solvent. The phosphorylated poly(vinyl alcohol) was characterized by  $^1H$  NMR,  $^{31}P$  NMR and FT-IR spectroscopy. Moreover, its thermal behaviour was investigated by TGA and DSC analysis.

### 2.5. Phosphorous quantification

To quantify the phosphorous amount in the PVA-based copolymers, alkalimetric titrations were carried out by an AMEL-338 pHmeter with Ag/AgCl glass electrode. The instrument calibration was obtained by two buffer solutions: potassium phosphate (pH = 7) and potassium hydrogen phthalate (pH = 4). NaOH solution (0.025 M) was used as a titrant. The samples were prepared by dissolving a defined amount of polymer (0.1 g) in 30 mL of distilled water and stirring for 3 days with NaCl salt in order to lead the acid protons in solution [39].

### 2.6. Characterization of polymers and CFRPs

The polymer structures were characterized and confirmed by  $^1H$  and  $^{13}C$  NMR spectroscopy, by using a Varian "Mercury 400" spectrometer, operating at 400 MHz. Tetramethylsilane (TMS) was used as an internal reference standard. The PPVA copolymers were also studied by  $^{31}P$  NMR using phosphoric acid ( $H_3PO_4$  85 % in water solution) as an external reference. Moreover, the polymers were characterized by FT-IR, acquiring the spectra by an ATR-IR Bruker Alpha I spectrometer. The samples' thermal stability was studied by TGA using a thermogravimetric apparatus (TA Instruments Q500) under a nitrogen atmosphere (flow rate 60 mL/min) at a 10 °C/min heating rate, from 25 °C to 600 °C. DSC analyses were performed with a TA Instrument Q2000, using unsealed aluminium pans, and loading 3 to 5 mg of sample. The DSC analyses were carried out by applying two subsequent heating ramps from -50 °C to 150 °C (heating/cooling ramps at 20 °C/min). SEM-EDX analysis was performed using a scanning electron microscope (SEM) ZEISS EVO 50 EP equipped with an energy-dispersive X-ray module for the element identification.

### 2.6.1. Cone-calorimeter tests on PPVA-coated CFRPs

Cone-calorimeter tests were carried out to evaluate the PPVA behaviour as a flame inhibitor and/or retardant. The tests were conducted via an oxygen consumption cone-calorimeter (FFT Cone Calorimeter, Fire Testing Technology) under an incident heat flux of 35 kW/m<sup>2</sup> (corresponding to a temperature of 670 °C, comparable to a small-scale fire scenario). The setup operates according to the ISO 5660 standard.

The dimension of each specimen was  $\approx 100 \times 100 \times 1.3$  mm. The measurements were carried out with the sample holder in horizontal orientation, without aluminium foil retainer wrap, using the edge frame but not the retainer grid. The distance between the sample surface and the cone-shaped heater was kept constant at 25 mm during the entire duration of the test. The cone-calorimeter test allows the assessment of the average heat release rate as a function of time-span (mean HRR), the peak of heat release rate (pHRR), and the total heat release (THR), all calculated as a function of the oxygen consumption. Moreover, it provides the time to ignition (TTI), the time of flame (TOF), and the time to pHRR (TTP).

The PPVA with the highest phosphorylation degree (7.5 % wt) has been selected to investigate the flame inhibitor property. First, a PPVA stock solution was prepared by solubilizing 2.5 g of PPVA in 29 mL of distilled water (8 % wt). Through further dilution, three additional solutions at lower concentrations, namely 1, 2, and 4 % wt were obtained. The polymeric solution was then poured onto the surface of the CFRP laminate (100 × 100 mm panels), previously cured in autoclave. Then, the PPVA-coated materials were placed on a heating plate at 80 °C to quickly evaporate the solvent and promote the homogeneous film formation on the substrate surface. The PPVA transparent film does not impact CFRP surface appearance nor leads to a statistically significant increase in the final laminate thickness, as displayed by histograms in Fig. 1.

The final PPVA coating grammage is 5, 10, 20 and 40 g/m<sup>2</sup>, using polymeric solutions at 1, 2, 5 and 8 % wt, respectively. For the sake of comparison, also plain PVA-coated specimens were produced and tested (by depositing the same amount of material as the previous ones), as well as uncoated CFRP plates. At least 3 test repetitions were performed for each specimen type to ensure the statistical significance of the results.

All the samples reported in Fig. 1 were tested at the cone-calorimeter. The reference CFRP laminate is called R-CP, where “R” stands for “Reference” and “CP” stands for “Composite Panel”. The CFRP laminates coated with PVA or PPVA are labelled CP-X\_PVA and CP-X\_PPVA\_7.5%, where “X” represents the coating grammage.

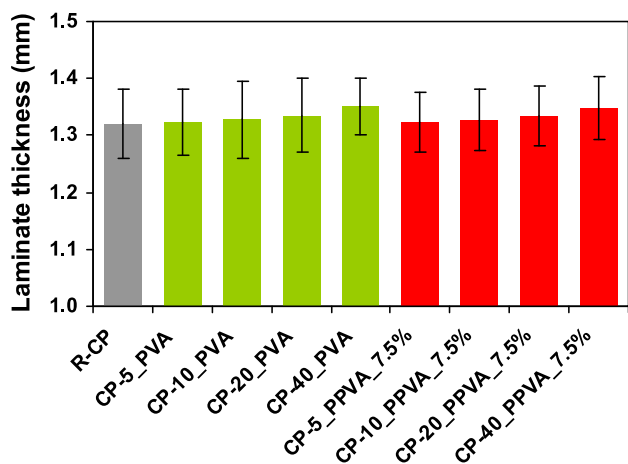


Fig. 1. Laminate thickness of samples for cone-calorimeter tests.

### 2.7. Kinetic analysis

To rationalize the degradation process and the mechanism involved during the combustion, several differential and integral isoconversional (free) models have been compared for evaluating the activation energy as a function of the degree of conversion (without assuming any kind of specific reaction mechanism). First, Friedman's equation (Eq. 1) was used [40,41]:

$$\ln\left(\beta \frac{d\alpha}{dT_\alpha}\right) = \ln(Af(\alpha)) - \frac{E_a}{RT_\alpha} \quad (1)$$

where  $\beta$  (K/min) is the heating rate;  $\alpha$  is the conversion degree ranging from 0 to 1;  $f(\alpha)$  is the reaction model,  $T_\alpha$  is the temperature as a function of the conversion degree ( $\alpha$ ) and  $R$  is the ideal gas constant (8.314 J/mol•K). The activation energy can be found from the slope of the curves obtained by plotting  $\ln\left(\beta \frac{d\alpha}{dT}\right)$  versus  $1/T$ , for each conversion value at different heating rates.

Another non-isothermal isoconversional differential approach is represented by the Kissinger-Akahira-Sunose (KAS) method, that by applying the Coats-Redfern approximation can be described by Eq. (2) [42–44]:

$$\ln\left(\frac{\beta}{T_\alpha^2}\right) = \ln\left(\frac{AR}{E_a g(\alpha)}\right) - \frac{E_a}{RT} \quad (2)$$

The terms present in the equation describe the same parameters previously reported, where  $g(\alpha)$  is the integral form of the kinetic model. The slope of the curve built by fitting  $\ln\left(\frac{\beta}{T_\alpha^2}\right)$  with the inverse of the temperature ( $1/T$ ) accounts for  $E_a$ .

The last method employed is the Flynn-Ozawa-Wall (FOW) integral isoconversional approach, which considers the trend of activation energy constant within the degradation process according to the following Eq. (3) where the Doyle approximation is applied [45–47]:

$$\ln\beta = \ln\left(\frac{AE_a}{Rg(\alpha)}\right) - 5.525 - 1.052 \frac{E_a}{RT_\alpha} \quad (3)$$

By plotting  $\ln\beta$  values deriving from thermal curves recorded at several heating rates versus  $1/T$  a straight curve was obtained, and the slope allows for the activation energy evaluation.

## 3. Results and discussion

Phosphorous compounds based on PVA were produced to obtain an intrinsically flame inhibitor polymeric film to be applied onto polymer composite materials to reduce their flammability. Indeed, while PVA polymer exhibits a limited oxygen index (LOI) of 19–20 % [48,49], it is demonstrated that the addition of phosphorous in the PVA macromolecular chain can raise the LOI above 21 %, making the polymer self-extinguishing [37,50]. For this reason, PVA-co-PPVA copolymers with different degrees of phosphorylation were synthesized by the post-polymerization reaction route reported in Fig. 2: firstly, polyvinyl acetate (PVAc) was polymerized from vinyl acetate (VAc) monomer, then the polymer was hydrolysed to PVA, and, finally, functionalised with phosphorous to obtain PPVA. Although the synthesis to produce such copolymers has already been reported in the literature [36,51], the amount of phosphorylated units achieved on the macromolecules has been increased thanks to the optimization of reaction parameters.

### 3.1. Synthesis and characterization of polymers

The structure of the synthesized polymers has been confirmed by NMR spectroscopy; the spectra of poly(vinyl acetate) (PVAc), poly(vinyl alcohol) (PVA) homopolymers and phosphorylated PVAs are reported in the Supplementary Information (Fig. S1). However, the <sup>1</sup>H NMR spectra of the phosphorylated polymers are quite similar to the functionalized PVA due to the absence of significant changes in terms of chemical shift

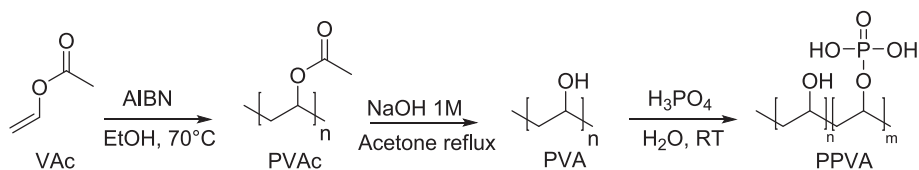


Fig. 2. Synthetic route for the preparation of poly(vinyl alcohol-co-vinyl alcohol phosphorylated) (PPVA).

related to the protons in the polymeric chain (Fig. S1). For this reason, to confirm the structure of the PPVA,  $^{31}\text{P}$  NMR experiments were carried out. In Fig. 3, the  $^{31}\text{P}$  NMR spectrum of PPVA\_7.5 % was reported, showing a single chemical shift at 1.28 ppm which can be attributed to phosphate monoesters, thus confirming the correct formation of a phosphorylated polymer [52]. Although the absence of an internal standard prevents a quantitative approach to determine the phosphorylation degree, all samples showed the signal related to phosphate monoester. In addition, the absence of other signals excludes a partial crosslinking among neighbouring phosphoric groups [36]. Despite crosslinking reaction involves the hydroxyl groups via condensation mechanism, by controlling reaction parameters, such as  $\text{H}_3\text{PO}_4$  concentration, temperature and reaction time, it was possible to obtain linear phosphorylated polymers with a relatively high functionalization degree. The lack of a 0 ppm signal accounts for the complete removal of the phosphoric acid used during the synthetic step. An analogue behaviour is observed for all the PVA-PPVA copolymers, whose spectra are not shown.

The phosphorylation degree was quantified by acid-base titration using NaOH (0.025 M) as a titrant. Analysing the titration curves (Fig. S2), the presence of two distinct equivalent points confirms the mono-ester product rather than the *pyro*-phosphoric ester stemming from the condensation reaction between neighbouring functionalized units, in agreement with  $^{31}\text{P}$  NMR spectra (Fig. 3). In order to evaluate the phosphorous amount contained in PPVA, only the first equivalent point was considered. A correlation is observed between the acid

concentration used during the phosphorylation step and the phosphorus

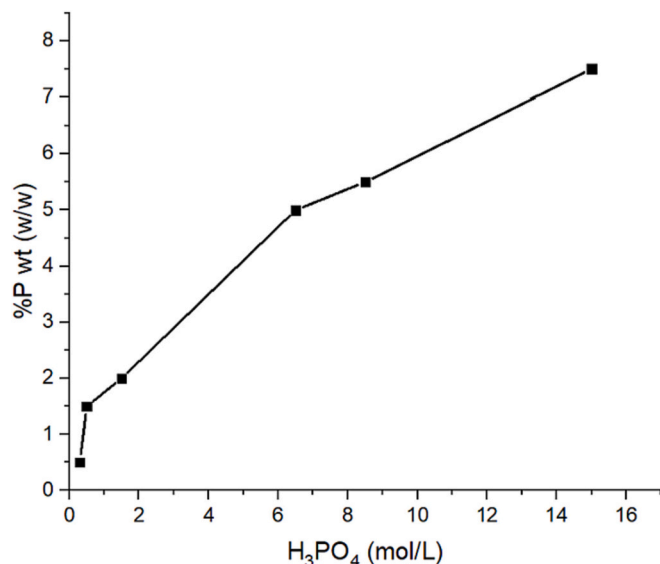


Fig. 4. Correlation between the phosphoric acid ( $\text{H}_3\text{PO}_4$ ) molarity with the degree of phosphorylation (%P wt).

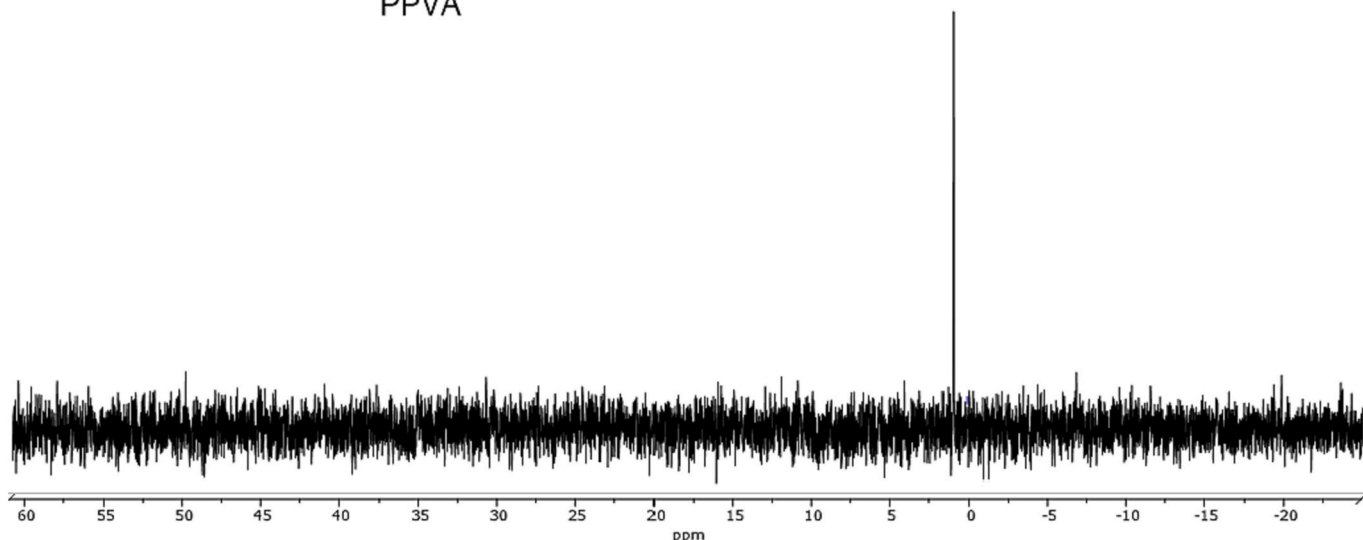
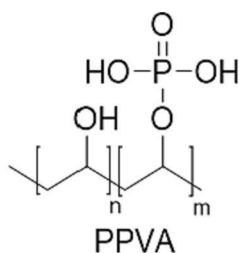


Fig. 3.  $^{31}\text{P}$  NMR spectra of PPVA\_7.5% in  $\text{D}_2\text{O}$  using phosphoric acid (85 %) as external standard.

weight percentage bonded on the polymeric chain (Fig. 4). Table 1 reports the average values normalized on the polymer weight.

FT-IR spectra of PVA-PPVA copolymers with different degrees of phosphorylation as well as the PVA homopolymer and the PVAc spectra are shown in full in Figs. S3–S4 of Supplementary Materials and compared. Hereafter, in Fig. 5 the 500–2000  $\text{cm}^{-1}$  spectral region is reported to observe the characteristic absorption peaks related to phosphorylated units. According to the PVA spectra reported in Supplementary Information, the strong absorbance at 1100  $\text{cm}^{-1}$  is related to C–O stretch and O–H bend which decreases in intensity in samples with the phosphorylated units, indicating the correct substitution of some of the C–OH bond by C–P–OH bond [53]. At the same time, the absorbance peak at 990  $\text{cm}^{-1}$ , characteristic of P–O stretching in alkyl phosphates and phosphite appeared in the copolymeric systems, with increased intensity when a higher amount of phosphorylated moieties are present. Thus, FT-IR spectra confirm that the synthesized PPVA polymers have different phosphorylation degrees (unphosphorylated alcoholic units are still present in all cases).

Thermogravimetric analyses were carried out to characterize the thermal stability of the synthesized PPVAs copolymers (Fig. 6). The thermograms were recorded in the 25–600 °C temperature range under a nitrogen atmosphere to evaluate the degradation profile as a function of the PVA phosphorylation degree.

The PVA homopolymer undergoes two different degradation steps: the first, around 300 °C, related to the degradation of the alcoholic moieties, and the second one near 420–450 °C, which is attributed to the thermal decomposition of the polymeric backbone [53].

Comparison (Fig. 6) of the PVA thermogram with those of PVA-co-PPVA copolymers clearly highlights significant differences in the thermo-degradative behaviour of the latter: the presence of phosphoric groups on the polymeric chain leads to a significant shift of the onset related to the first decomposition stage ( $T_d$ ) more and more toward lower temperatures as the P content in the polymer increases (Table 2).

Moreover, the residue becomes higher by increasing the PVA degree of phosphorylation, highlighting a strong charring ability that increases with P content [51,54]. This behaviour can be explained by the presence of phosphoric units that at the beginning of the degradation undergo intramolecular elimination, followed by a condensation step between phosphoric moieties and therefore the formation of crosslinked units that prevent the subsequent degradative phase leading to a solid residue.

As reported in Fig. 7, a correlation was observed between the degree of phosphorylation and the degradation temperature ( $T_d$ ) of the polymer: the degradation step starts at a lower temperature when the phosphorylated amount increases [54]. Since charring ability has often been reported as a symptom of good intumescent properties, the impressive charring ability obtained already with a few percentages of P suggests a possible use of PPVA as a flame inhibitor agent, acting as an intumescent barrier [55,56].

The DSC thermograms of phosphorylated PPVAs, as well as the PVA homopolymer, are reported in Fig. S6. The midpoint of the step-change was used to evaluate the glass transition temperature ( $T_g$ ). A shift of the polymer glass transition toward lower temperatures was observed as the amount of phosphorous in PPVA increased. The  $T_g$ , centred at 82 °C for the unfunctionalized PVA, reaches 54 °C for the PPVA with 7.5 % wt of phosphorous, as indeed expected based on the self-plasticization ability

**Table 1**  
Phosphorus amount in copolymeric system evaluated by alkalimetric titration.

Sample	H <sub>3</sub> PO <sub>4</sub> (mol/L)	%P wt	%P mol
PVA	–	–	–
PPVA_0.5%	0.3	0.5	0.8
PPVA_1.5%	0.5	1.5	1.9
PPVA_2%	1.5	2.0	2.9
PPVA_5%	6.5	5.0	7.0
PPVA_5.5%	8.5	5.5	8.0
PPVA_7.5%	15.0	7.5	12.5

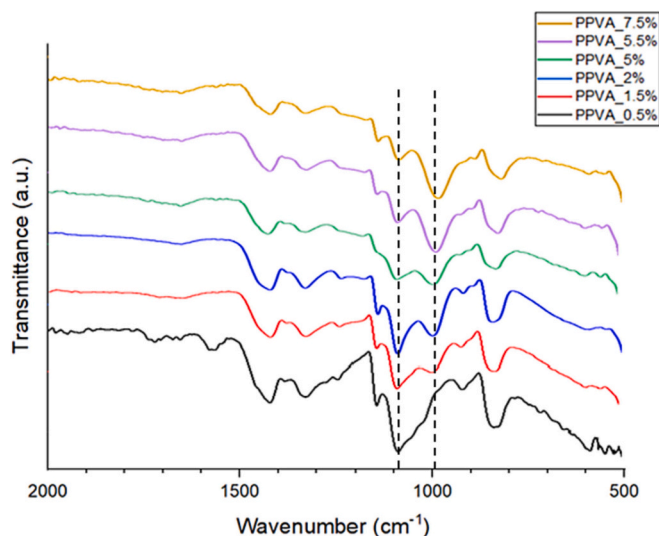


**Fig. 5.** FT-IR spectra (500–2000  $\text{cm}^{-1}$ ) of poly(vinyl alcohol-co-vinyl alcohol phosphorylated) (PPVA) copolymers with different composition.

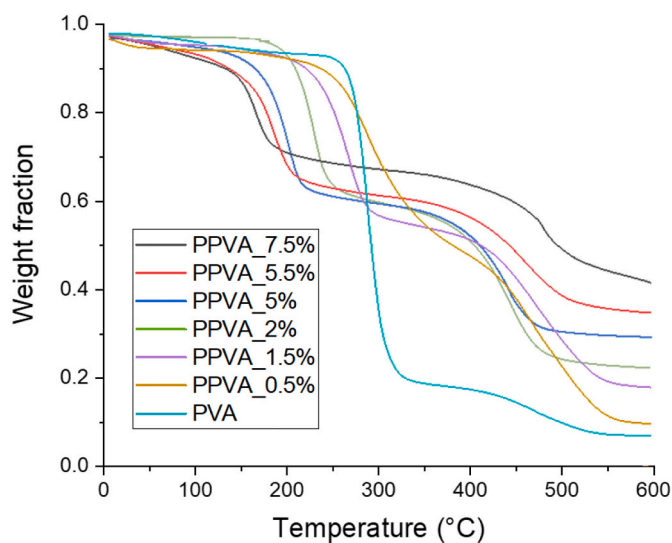


**Fig. 6.** Thermogravimetric analysis (TGA) of PVA and PPVA with different amounts of phosphorus.

**Table 2**  
Degradation temperature ( $T_d$ ) and residue percentage of PVA and PPVA with different amounts of phosphorus.

Sample	$T_d$ (°C)*	Residue (%wt)
PVA	300	6.9
PPVA_0.5%	290	9.7
PPVA_1.5%	275	17.9
PPVA_2%	240	22.1
PPVA_5%	215	29.8
PPVA_5.5%	200	31.1
PPVA_7.5%	190	34.8

\* Degradation temperature was evaluated considering the weight loss onset on TGA curves.

of the bulky phosphorylated moieties with respect to the plain, unmodified, free hydroxyl groups. However, the overlapping of the melting and degradation temperature limited the investigation of the thermal behaviour in the higher temperature range.

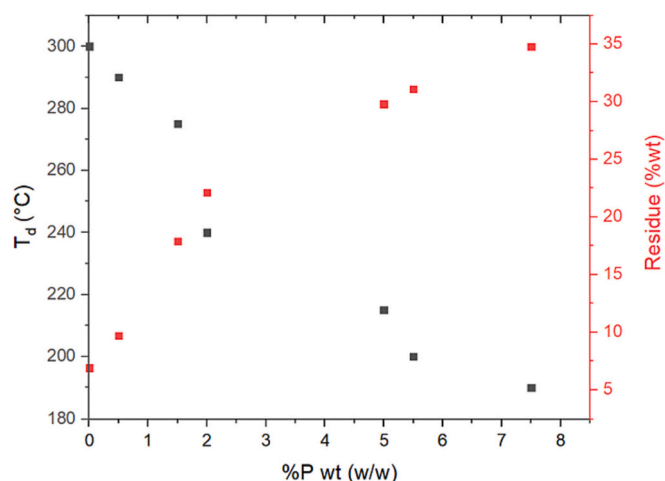


Fig. 7. Correlation between the residue (black points) and the degradation temperature,  $T_d$ , (red points) as a function of the phosphorous weight percentage in PPVA. (For interpretation of the references to color in this figure legend, the reader is referred to the web version of this article.)

### 3.2. Thermal degradation kinetics

To investigate the thermal degradation kinetics, TGA curves of the pure PVA and PPVA\_7.5% at different heating rates (20, 30, 40 and 50 °C/min) were recorded under a nitrogen atmosphere. The PPVA with the maximum degree of phosphorylation (7.5 % wt P) was chosen to test samples with the greatest differences in terms of composition and to emphasize the different degradation behaviours. For this purpose, the three different methodologies described in the Experimental section were employed and compared to investigate the thermo-kinetic parameters and therefore rationalize the degradation mechanism.

In particular, Flynn-Ozawa-Wall (FOW), Friedman and Kissinger-Akahira-Sunose (KAS) methods are applied. The use of complementary methods is required when a multi-steps reaction pathway is involved. In general, integral FOW's method is the more appropriate approach to describe complex kinetic phenomena than the differential Friedman and KAS's models [40,57]. However, when consecutive reactions or reactions with a high difference in terms of activation energy simultaneously occur, the method could be unsuitable for the purpose so a differential approach can be favourite [58]. Besides the described drawbacks in modelling complex reactions, when independent reactions are involved the comparison of different approaches should lead to the same results. Herein, the fitted curves and the thermodynamic parameters are reported in Fig. S7 and Table 3, respectively.

Table 3

Activation energy ( $E_a$ ) and R square values calculated for the PVA and PPVA\_7.5% samples by applying FOW, Friedman and KAS methods.

	$\alpha$	FOW		Friedman		KAS	
		$E_a$ (kJ/mol)	$R^2$	$E_a$ (kJ/mol)	$R^2$	$E_a$ (kJ/mol)	$R^2$
PVA	0.1	232.4	0.82	235.7	0.81	226.9	0.80
	0.2	135.7	0.93	133.6	0.92	124.6	0.91
	0.3	119.9	0.98	105.8	0.89	107.6	0.98
	0.4	91.8	0.98	88.1	0.97	79.6	0.97
	0.5	83.4	0.99	77.9	0.98	69.2	0.98
	0.6	79.9	0.99	75.3	0.99	66.4	0.98
	0.7	80.8	0.95	75.7	0.89	66.5	0.97
Average		117.7		113.2		105.8	
PPVA_7.5%	0.1	30.4	0.97	28.1	0.96	24.2	0.97
	0.2	32.5	0.99	30.1	0.98	26.1	0.99
	0.3	141.8	0.96	144.9	0.92	140.6	0.96
	0.4	43.6	0.99	51.4	0.99	57.1	0.99
	0.5	186.9	0.91	202.8	0.84	208.9	0.91
	0.6	55.1	0.96	64.7	0.94	71.4	0.96
Average		81.7		87.0		88.1	

By analysing the curves reported in Fig. S7, a good fitting, as described by  $R^2$  values, can be observed for each sample. The activation energy calculated for the pure PVA thermal degradation was 117.7, 113.2 and 105.8 kJ derived from the application of FOW, Friedman and KAS methods, respectively. Instead, PPVA\_7.5 % has highlighted different results: 81.7 kJ (FOW), 87.0 kJ (Friedman) and 88.1 kJ (KAS). A slight difference was observed comparing the activation energies evaluated by differential and integral methods due to the temperature integrals approximations employed during the derivation of the equations [43]. In the case of PVA, the values obtained by using the KAS and Friedman approaches were lower than the results related to FOW's method. Instead, for the PPVA sample, the  $E_a$  calculated by the integral method is lower if compared to the others. To better rationalize the phenomena, the relationship between  $E_a$  and the conversion degree ( $\alpha$ ) was also investigated and reported in Fig. 8. In both samples there is no direct proportionality of the two parameters, thus suggesting the presence of several consecutive reactions during the degradation phase. In the case of PVA, the activation energy decreases as a function of  $\alpha$  in agreement with the literature [59]. Instead, the PPVA trend exhibited a segmented trend, with alternate low and high activation energy values. Such an irregular trend of the activation energy can be explained by the presence of different degradative steps during the process. The presence of the first maximum can be explained by the phosphorus tendency to couple the radicals formed during the combustion inhibiting the process and limiting the complete degradation of the substrate [24]. In this way, by a thermo-kinetic approach we have demonstrated the role of the phosphorous as inhibitor agent during the degradation mechanism.

### 3.3. Fire testing of PPVA-coated CFRPs

To evaluate the behaviour of the PVA and 7.5% phosphorylated PPVA as flame inhibitor coatings for composite materials, different samples were prepared and tested at the cone-calorimeter. The tests were carried out with an incident heat flux of 35 kW/m<sup>2</sup>, corresponding to a small-scale fire event [60]. The instrument can operate with a heat flow in the 5–100 kW/m<sup>2</sup> range. While an irradiation power above 50 kW/m<sup>2</sup> simulates a fully developed fire and provides better data reproducibility and shorter measurement times, weaker irradiation levels, instead, are more suitable for fire protection goals. Indeed, under a heat flux of 35 kW/m<sup>2</sup> the test evaluates the material behaviour in conditions reminiscent of the beginning of a fire, where single components could contribute to flames spreading, thus demonstrating the intrinsic material's ability to ignite and propagate. The representative HRR vs. time curves and results are shown in Fig. 9 and listed in Table 4.

As clearly reported in Fig. 9 and Table 4, the presence of a PPVA coating, at any grammage, plays a relevant role in the flame inhibitor action. All the PPVA films perform better than the uncoated material

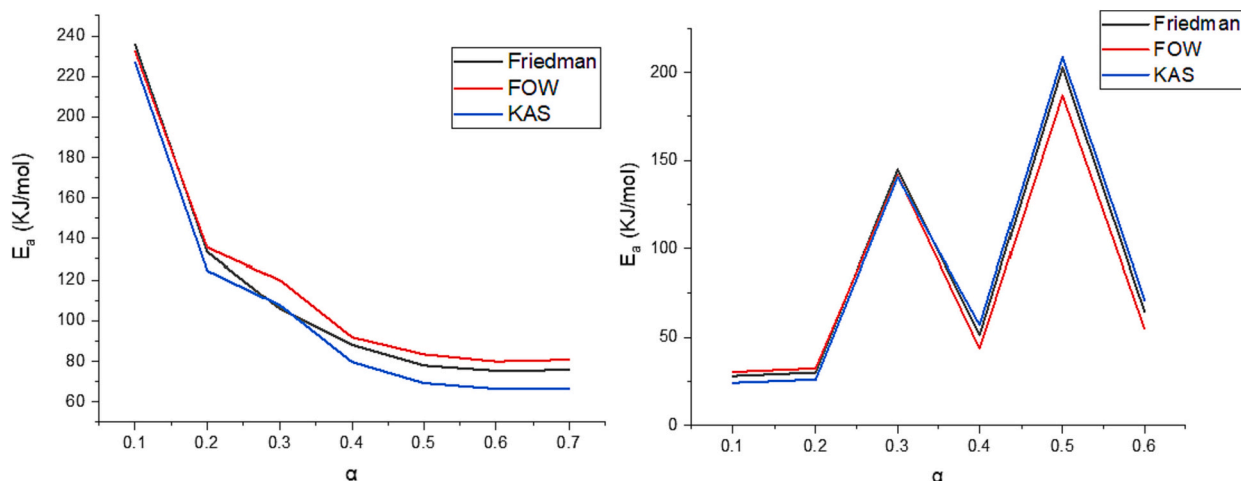


Fig. 8. Activation energy trend as a function of conversion degree for PVA and PPVA\_7.5%.

(R-CP) in terms of HRR, with a moderate decreasing trend obtained by increasing the amount of PPVA\_7.5 %, in particular for the CP-40\_PPVA\_7.5 %, where a 30 % decrease was achieved with respect to the plain composite. Regarding the pHRR values, very similar results are observed, without a significant impact of the PPVA coating on the overall behaviour of the samples. Similar results were also observed for the time to peak (TTP) values, where all the samples showed a very slight TTP decrease than the reference. Total heat release (THR) values confirm the trend observed with the HRR, with a drop of such parameter upon increasing the grammage, reaching a considerable decrease in the THR up to  $-28$  % (sample CP-40\_PPVA\_7.5 %). As suggested also by TGA measurements, the presence of phosphate groups undergoing crosslinking reaction tends to anticipate thermo-degradation, hence time to ignition (TTI) values for PPVA-coated samples are slightly shorter than P-free counterparts. Such differences, however, are not as outstanding as could be expected taking into account the TGA thermograms (Fig. 6), where a relevant decrease in the degradation temperature ( $T_d$ ), evaluated as the onset temperature of significant weight loss, is observed for increasing the phosphorylation degree.

PPVA coatings provide the most significant enhancement in the time of flame (TOF): in all cases, an average decrease of at least 50 %, compared to the uncoated composite, was achieved ( $-58$  % for the sample CP-40\_PPVA\_7.5 %). This supports the hypothesis that a charring residue, formed immediately after the beginning of the fire (Fig. 10C), promotes flame extinction faster than P-free materials, thus increasing the intrinsic safety of the composite panels in a hypothetical fire scenario. SEM-EDX investigation can be useful for evaluating the distribution of the elements on the surface exposed to the heating source during fire tests [61]. PPVA-coated laminates reveal that P lies mostly in the char residue (6.1 % by weight). However, a homogeneous distribution of P can also be detected on the carbon fibers, as displayed by EDX mapping (Fig. 10F). The charring ability of the phosphoric moieties is also observed to hamper the weight loss of samples, returning residues at the end of the test that are quite compact. While it is, indeed, expected that the composite would predominantly degrade with the loss of the matrix (33 % wt based on the prepreg composition), the carbonaceous fiber-based residue is expected to remain in mild fire conditions [7]. Indeed, in the plain composite, a weight loss ( $\approx 34$  % wt) comparable to the resin fraction is detected, while the addition of a PPVA coating limits this phenomenon: a mass loss lower than the expected resin fraction is recorded, in particular in the case of CP-40\_PPVA\_7.5 % ( $\approx 28$  % wt of weight loss). The fact that some matrix, even if strongly altered and damaged, is still able to remain within the fibrous residue would suggest that the coated panel could guarantee also better mechanical resistance during the fire.

Furthermore, as shown in Fig. 10A–B, the surface treatment does not affect the surface colour (with also no significant increase in the final thickness, Fig. 1) of the material, which retains its “carbon look”.

Completely different considerations can be drawn for PVA-coated composite material (CP-5\_PVA). Indeed, PVA significantly worsens the material’s flame behaviour: such coating increases the HRR and THR, besides a 30 % boost in TOF, which makes the material less safe in a fire scenario. In the histograms of Fig. 9 only the CP-5\_PVA sample was included, since increasing the grammage from  $5 \text{ g/m}^2$  to  $40 \text{ g/m}^2$  did not alter the overall fire behaviour (the results obtained for all the PVA-coated samples are reported in the Supplementary information, Fig. S8 and Table S1).

Considering the above-discussed results, it is possible to affirm that PPVA coatings applied on polymeric matrix composites provide a significant flame inhibitor capability, contributing to making the composite material safer in a fire scenario.

#### 4. Conclusions

The present work proposes PPVA as a flame-inhibitor coating for polymeric composite materials, using epoxy-based CFRP laminates as substrate.

PPVAs with high phosphorylation degrees, up to 7.5 % wt, without the presence of crosslinked units were obtained by post-polymerization functionalization of poly(vinyl alcohol) (PVA). The synthesized PPVAs were characterized by different spectroscopic and thermal analyses to confirm the right functionalization and to evaluate their thermal behaviour: a good linear correlation between the preparation condition and the final P-content was found, thus allowing for a tailored functionalization degree. Preliminary thermogravimetric analysis (TGA) on produced PPVAs revealed their strong charring ability, which becomes more effective by increasing the number of phosphorylated moieties, thus confirming the beneficial effect of phosphorus under flame conditions. In addition, coatings with different grammages (5, 10, 20 and  $40 \text{ g/m}^2$ ) were applied on CFRP laminates by solvent casting. The surface coating has no important effects on the material surface appearance, which retains its “carbon look”, nor a significant increase of the final laminate thickness.

Cone-calorimeter tests were carried out on both coated and uncoated materials for simulating a small-scale fire scenario. Results reveal that the laminates protected with PPVA exhibit a decreased time of flame (TOF), total heat release (THR) and weight loss with respect to uncoated and PVA-coated samples, confirming the flame inhibitor ability of PPVA. In particular, in the best case (represented by a sample coated with PPVA with a phosphorylation degree of 7.5 %), data evidence a halved TOF

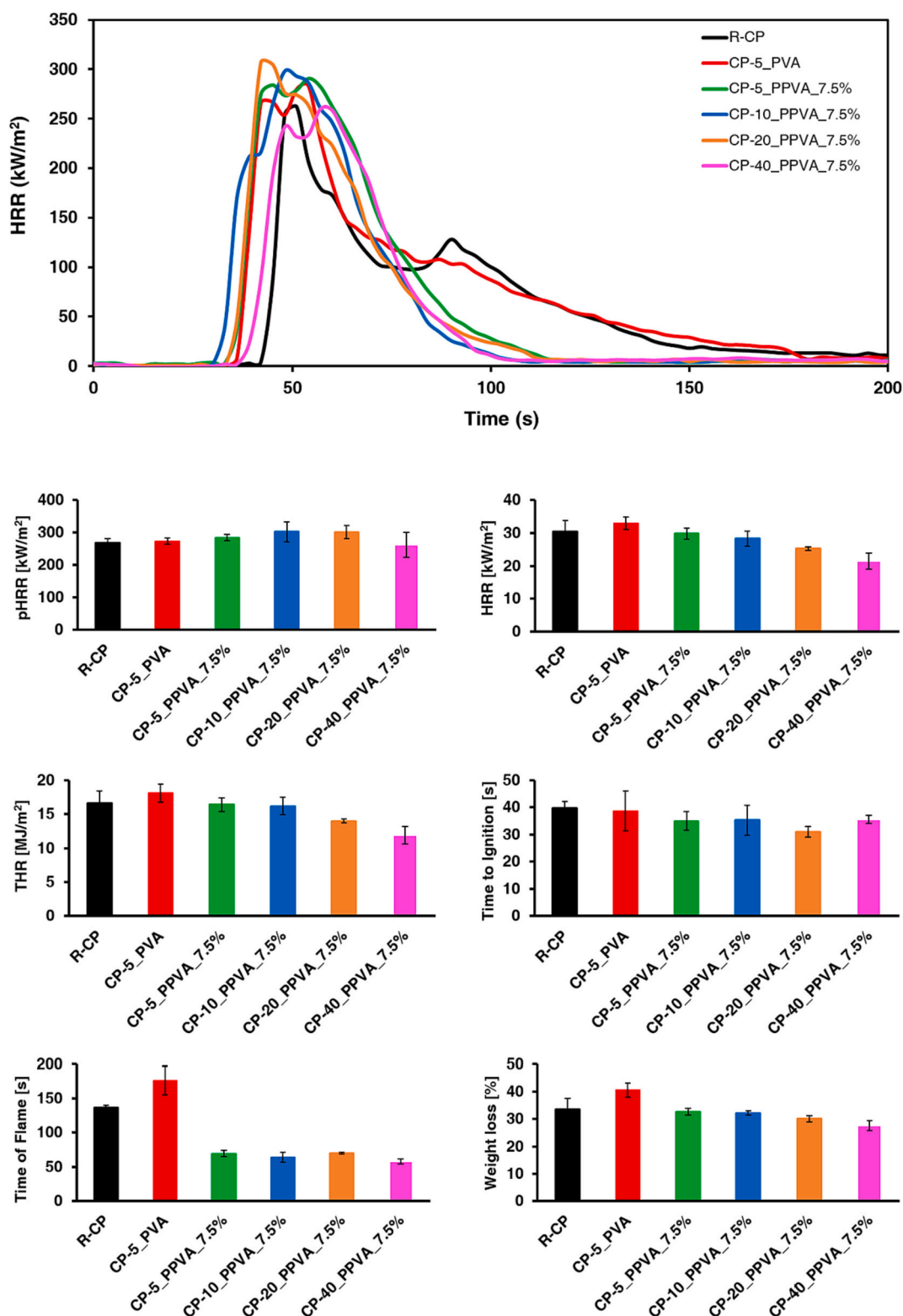


**Fig. 9.** Representative HRR vs. time curves and cone-calorimeter histograms for samples tested at the cone-calorimeter: pHRR, mean HRR, THR, time to ignition, time of flame and weight loss versus grammage. Colours: R-CP (uncoated CFRP, in black), CP-5\_PVA (PVA 5 g/m<sup>2</sup>, in red), CP-5\_PPVA\_7.5% (PPVA 5 g/m<sup>2</sup>, in green), CP-10\_PPVA\_7.5% (PPVA 10 g/m<sup>2</sup>, in blue), CP-20\_PPVA\_7.5% (PPVA 20 g/m<sup>2</sup>, in orange) and CP-40\_PPVA\_7.5% (PPVA 40 g/m<sup>2</sup>, in fuchsia). (For interpretation of the references to colour in this figure legend, the reader is referred to the web version of this article.)

(−58 %), a reduction of 28 % in THR, and −18 % in weight loss. The use of a PVA coating, instead, leads to a general worsening of all the fire parameters (+28 % in TOF, +9 % in THR and +21 % in weight loss).

To rationalize the reason why the time to ignition (TTI) decreased

with the P-containing coatings, thermo-degradative kinetics were studied, thus finding a correlation between activation energy and conversion degree. The decreasing activation energy justifies the TTI values, confirming the phosphorus catalytic effect, while the  $E_a$  profile of



**Table 4**

Flame behaviour of composite panels uncoated, coated with PVA and with different grammages of PPVA films containing a 7.5 % wt of P, determined by cone-calorimeter measurements.

Sample	HRR <sup>a</sup> (kW/m <sup>2</sup> )	pHRR <sup>b</sup> (kW/m <sup>2</sup> )	TTP <sup>c</sup> (s)	THR <sup>d</sup> (MJ/m <sup>2</sup> )	TTI <sup>e</sup> (s)	TOF <sup>f</sup> (s)	W. L. <sup>g</sup> (%)
R-CP	30.6 ± 3.3	268 ± 13	55 ± 10	16.6 ± 1.8	40 ± 3	137 ± 4	33.7 ± 3.8
CP-5_PVA	33.1 ± 1.9	274 ± 9	56 ± 12	18.1 ± 1.3	39 ± 7	176 ± 21	40.7 ± 2.6
CP-5_PPVA_7.5%	29.9 ± 1.7	285 ± 10	53 ± 2	16.4 ± 1.0	35 ± 4	69 ± 5	32.7 ± 1.2
CP-10_PPVA_7.5%	28.4 ± 2.3	303 ± 31	52 ± 5	16.2 ± 1.3	35 ± 6	64 ± 7	32.3 ± 0.8
CP-20_PPVA_7.5%	25.3 ± 0.5	302 ± 21	40 ± 2	14.0 ± 0.3	31 ± 5	70 ± 2	30.1 ± 1.1
CP-40_PPVA_7.5%	21.5 ± 2.5	263 ± 39	51 ± 5	11.9 ± 1.3	36 ± 2	58 ± 4	27.7 ± 1.8

<sup>a</sup> Average heat release rate (HRR) is the irradiated thermic power released by the sample per square meter.

<sup>b</sup> Peak heat release rate (pHRR) is the higher value of HRR.

<sup>c</sup> Time to peak (TTP) is the time required to pHRR.

<sup>d</sup> Total heat release (THR) is the total heat released by the sample during the entire duration of the test.

<sup>e</sup> Time to ignition (TTI) is the time needed for the first flame detection.

<sup>f</sup> Time of flame (TOF) is the flame lifetime.

<sup>g</sup> Weight loss (W. L.) is the amount of mass loss during the test.

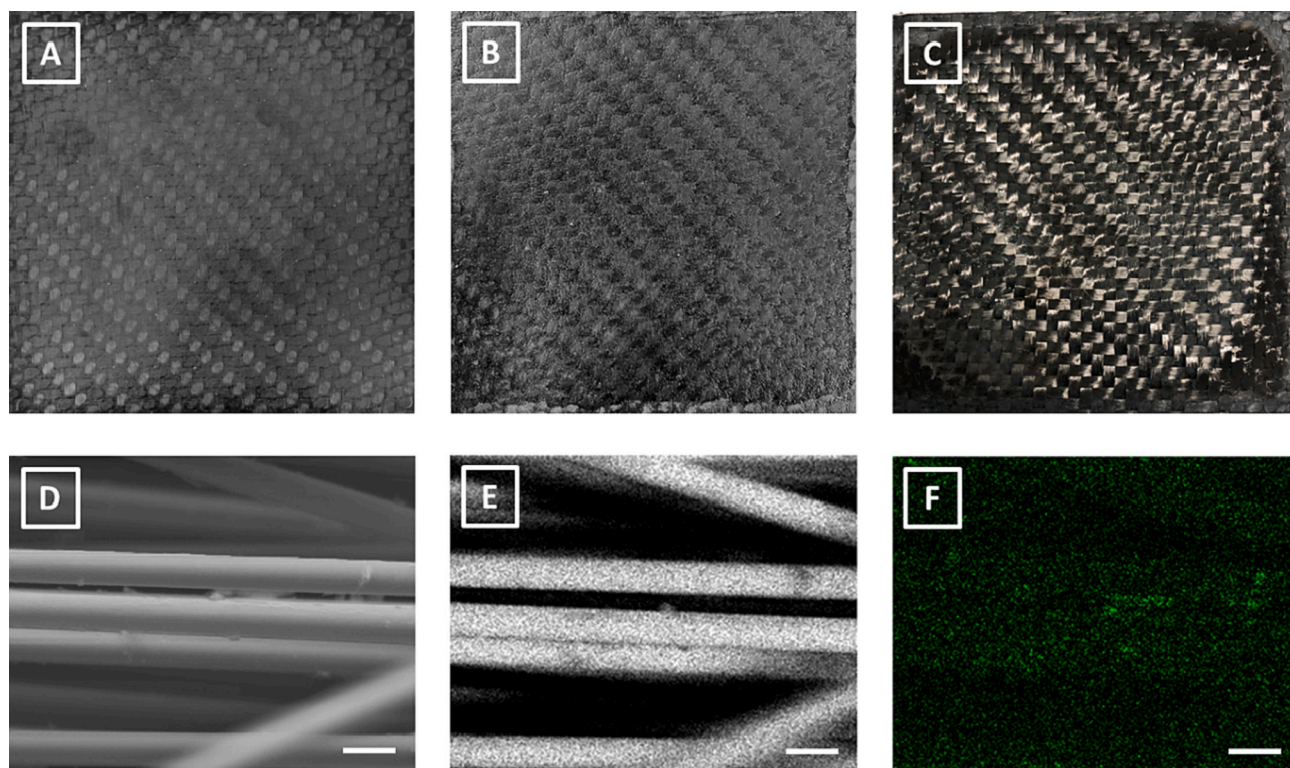


**Fig. 10.** (Top) Cone-calorimeter specimens: (A) before the application of a PVA or PPVA coating; (B) after the application of the polymeric coating; (C) after cone-calorimeter test. (Bottom) SEM-EDX investigation after cone-calorimeter tests: (D) SEM image of carbon fibers; EDX map highlighting (E) the carbon and (F) phosphorus distribution in the same analyzed region displayed in (D). Scale bars: 10  $\mu\text{m}$ .

PPVA\_7.5% polymer highlights its radicals-coupling behaviour.

The results highlight the active role of the PPVA polymer as a flame inhibitor, paving the way to the use of PPVA coatings to reduce the fire risk of composite laminates.

#### CRedit authorship contribution statement

Conceptualization, S.S., J.O., A.G.; data curation, S.S., J.O., A.G and E.M.; formal analysis, J.O. and A.G.; investigation, S.S., J.O., A.G.; methodology, S.S., J.O. and E.M.; project administration, D.C. and L.M.; supervision, D.C. and L.M.; validation, S.S. and J.O.; visualization, S.S., J.O. and E.M.; writing—original draft preparation, S.S. and J.O.; writing—review and editing, S.S., J.O., A.G., E.M., D.C. and L.M. All authors have read and agreed to the published version of the manuscript.

#### Declaration of competing interest

The authors declare that they have no known competing financial interests or personal relationships that could have appeared to influence the work reported in this paper.

#### Data availability

The raw/processed data required to reproduce these findings cannot be shared at this time as the data also forms part of an ongoing study.

#### Acknowledgements

The present work was funded under the National Recovery and Resilience Plan (NRRP), Mission 04 Component 2 Investment 1.5 –

NextGenerationEU, Call for tender n. 3277 dated 30/12/2021. Award Number: 0001052 dated 23/06/2022.

## Appendix A. Supplementary data

Supplementary data to this article can be found online at <https://doi.org/10.1016/j.porgcoat.2023.107457>.

## References

- [1] D.K. Rajak, D.D. Pagar, R. Kumar, C.I. Pruncu, Recent progress of reinforcement materials: a comprehensive overview of composite materials, *J. Mater. Res. Technol.* 8 (2019) 6354–6374, <https://doi.org/10.1016/j.jmrt.2019.09.068>.
- [2] R.C. Thompson, S.H. Swan, C.J. Moore, F.S. vom Saal, Our plastic age, *Philos. Trans. R. Soc. B Biol. Sci.* 364 (2009) 1973–1976, <https://doi.org/10.1098/rstb.2009.0054>.
- [3] N. Saba, M. Jawaid, M.T. Paridah, O.Y. Al-othman, A review on flammability of epoxy polymer, cellulosic and non-cellulosic fiber reinforced epoxy composites: flammability of epoxy polymer and its composites, *Polym. Adv. Technol.* 27 (2016) 577–590, <https://doi.org/10.1002/pat.3739>.
- [4] F. Uddin, Flame-retardant fibrous materials in an aircraft, *J. Ind. Text.* 45 (2016) 1128–1169, <https://doi.org/10.1177/1528083714540700>.
- [5] R.A. Mensah, V. Shanmugam, S. Narayanan, J.S. Renner, K. Babu, R.E. Neisiany, M. Försth, G. Sas, O. Das, A review of sustainable and environment-friendly flame retardants used in plastics, *Polym. Test.* 108 (2022), 107511, <https://doi.org/10.1016/j.polymertesting.2022.107511>.
- [6] A.P. Mouritz, S. Feih, E. Kandare, Z. Mathys, A.G. Gibson, P.E. Des Jardin, S. W. Case, B.Y. Lattimer, Review of fire structural modelling of polymer composites, *Compos. Part Appl. Sci. Manuf.* 40 (2009) 1800–1814, <https://doi.org/10.1016/j.compositesa.2009.09.001>.
- [7] L. Mazzocchetti, T. Benelli, E. Maccaferri, S. Merighi, J. Belcarì, A. Zucchelli, L. Giorgini, Poly-m-aramid electrospun nanofibrous mats as high-performance flame retardants for carbon fiber reinforced composites, *Compos. Part B Eng.* 145 (2018) 252–260, <https://doi.org/10.1016/j.compositesb.2018.03.036>.
- [8] A.B. Morgan, J.W. Gilman, An overview of flame retardancy of polymeric materials: application, technology, and future directions, *Fire Mater.* 37 (2013) 259–279, <https://doi.org/10.1002/fam.2128>.
- [9] S. Liu, V.S. Chevali, Z. Xu, D. Hui, H. Wang, A review of extending performance of epoxy resins using carbon nanomaterials, *Compos. Part B Eng.* 136 (2018) 197–214, <https://doi.org/10.1016/j.compositesb.2017.08.020>.
- [10] A. Cingolani, R. Mazzoni, V. Zanotti, M. Sanviti, L. Mazzocchetti, T. Benelli, L. Giorgini, Bis-amino functionalized iron N-heterocyclic carbene as epoxy resins hardener and flame behaviour modifier, in: *Ischia, Italy, 2019*, p. 020035, <https://doi.org/10.1063/1.5140308>.
- [11] Z.X. Zhang, J. Zhang, B.-X. Lu, Z.X. Xin, C.K. Kang, J.K. Kim, Effect of flame retardants on mechanical properties, flammability and foamability of PP/wood-fiber composites, *Compos. Part B Eng.* 43 (2012) 150–158, <https://doi.org/10.1016/j.compositesb.2011.06.020>.
- [12] S. Merighi, E. Maccaferri, J. Belcarì, A. Zucchelli, T. Benelli, L. Giorgini, L. Mazzocchetti, Interaction between polyaramidic electrospun nanofibers and epoxy resin for composite materials reinforcement, in: *Adv. Mater. Eng. Mater. VI*, Trans Tech Publications Ltd, 2017, pp. 39–44, <https://doi.org/10.4028/www.scientific.net/KEM.748.39>.
- [13] R. Jeenchan, N. Suppakarn, K. Jarukumjorn, Effect of flame retardants on flame retardant, mechanical, and thermal properties of sisal fiber/polypropylene composites, *Compos. Part B Eng.* 56 (2014) 249–253, <https://doi.org/10.1016/j.compositesb.2013.08.012>.
- [14] S. Liang, N.M. Neisius, S. Gaan, Recent developments in flame retardant polymeric coatings, *Prog. Org. Coat.* 76 (2013) 1642–1665, <https://doi.org/10.1016/j.porgcoat.2013.07.014>.
- [15] Q. Wu, Q. Zhang, L. Zhao, S.-N. Li, L.-B. Wu, J.-X. Jiang, L.-C. Tang, A novel and facile strategy for highly flame retardant polymer foam composite materials: transforming silicone resin coating into silica self-extinguishing layer, *J. Hazard. Mater.* 336 (2017) 222–231, <https://doi.org/10.1016/j.jhazmat.2017.04.062>.
- [16] Y.-Y. Yen, H.-T. Wang, W.-J. Guo, Synergistic flame retardant effect of metal hydroxide and nanoclay in EVA composites, *Polym. Degrad. Stab.* 97 (2012) 863–869, <https://doi.org/10.1016/j.polymdegradstab.2012.03.043>.
- [17] M. Joulaei, K. Hedayati, D. Ghanbari, Investigation of magnetic, mechanical and flame retardant properties of polymeric nanocomposites: green synthesis of MgFe<sub>2</sub>O<sub>4</sub> by lime and orange extracts, *Compos. Part B Eng.* 176 (2019), 107345, <https://doi.org/10.1016/j.compositesb.2019.107345>.
- [18] G. Vahidi, D.S. Bajwa, J. Shojaeiarani, N. Stark, A. Darabi, Advancements in traditional and nanosized flame retardants for polymers—a review, *J. Appl. Polym. Sci.* 138 (2021) 50050, <https://doi.org/10.1002/app.50050>.
- [19] B. Schartel, B. Perret, B. Ditttrich, M. Ciesielski, J. Krämer, P. Müller, V. Altstädt, L. Zang, M. Döring, Flame retardancy of polymers: the role of specific reactions in the condensed phase, *Macromol. Mater. Eng.* 301 (2016) 9–35, <https://doi.org/10.1002/mame.201500250>.
- [20] B.K. Kandola, K.V. Williams, J.R. Ebdon, Organo-inorganic hybrid intumescent fire retardant coatings for thermoplastics based on poly(vinylphosphonic acid), *Molecules* 25 (2020) 688, <https://doi.org/10.3390/molecules25030688>.
- [21] W. Wang, H. Li, Q. Li, Z. Luo, A novel grafted polyethylene with diphenyl phosphoryl group: improved flame retardancy and favorable compatibility, *J. Appl. Polym. Sci.* 138 (2021) 51242, <https://doi.org/10.1002/app.51242>.
- [22] E. Gallo, B. Schartel, D. Acierno, P. Russo, Flame retardant biocomposites: synergism between phosphinate and nanometric metal oxides, *Eur. Polym. J.* 47 (2011) 1390–1401, <https://doi.org/10.1016/j.eurpolymj.2011.04.001>.
- [23] L. Macarie, G. Ilia, Poly(vinylphosphonic acid) and its derivatives, *Prog. Polym. Sci.* 35 (2010) 1078–1092, <https://doi.org/10.1016/j.progpolymsci.2010.04.001>.
- [24] P. Joseph, S. Tretsiakova-McNally, Reactive modifications of some chain- and step-growth polymers with phosphorus-containing compounds: effects on flame retardance—a review: chemical modifications of polymers, *Polym. Adv. Technol.* 22 (2011) 395–406, <https://doi.org/10.1002/pat.1900>.
- [25] R. Shree, R.B. Naik, G. Gunasekaran, Phytic acid based novel optically transparent intumescent fire-retardant coating for protection of combustible substrates with retention of aesthetic appearance, *J. Coat. Technol. Res.* (2021), <https://doi.org/10.1007/s11998-021-00537-2>.
- [26] L. Yan, X. Tang, X. Xie, Z. Xu, Fire resistance, thermal and anti-ageing properties of transparent fire-retardant coatings modified with different molecular weights of polyethylene glycol borate, *Polymers* 13 (2021) 4206, <https://doi.org/10.3390/polym13234206>.
- [27] K. Williams, J.R. Ebdon, B.K. Kandola, Intumescent fire-retardant coatings for plastics based on poly(vinylphosphonic acid): improving water resistance with comonomers, *J. Appl. Polym. Sci.* 137 (2020) 47601, <https://doi.org/10.1002/app.47601>.
- [28] G. Malucelli, F. Carosio, J. Alongi, A. Fina, A. Frache, G. Camino, Materials engineering for surface-confined flame retardancy, *Mater. Sci. Eng. R Rep.* 84 (2014) 1–20, <https://doi.org/10.1016/j.mser.2014.08.001>.
- [29] S. Merighi, L. Mazzocchetti, T. Benelli, E. Maccaferri, A. Zucchelli, A. D'Amore, L. Giorgini, A new wood surface flame-retardant based on poly-m-aramid electrospun nanofibers, *Polym. Eng. Sci.* 59 (2019) 2541–2549, <https://doi.org/10.1002/pen.25235>.
- [30] J. Li, W. Tong, L. Yi, Flame-retardant composite coatings for cotton fabrics fabricated by using oxygen plasma-induced polymerization of vinyl phosphonic acid/cyclohexylsiloxane, *Text. Res. J.* 89 (2019) 5053–5066, <https://doi.org/10.1177/0040517519848158>.
- [31] A. Beaugendre, S. Saidi, S. Degoutin, S. Bellayer, C. Pierlot, S. Duquesne, M. Casetta, M. Jimenez, One pot flame retardant and weathering resistant coatings for plastics: a novel approach, *RSC Adv.* 7 (2017) 40682–40694, <https://doi.org/10.1039/C7RA08028J>.
- [32] Y. Dou, X. Li, K. Zheng, J. Liu, J. Hou, Study on curing and flammability properties of UV-curable flame-retardant coating on jute/polypropylene composites surface, *J. Therm. Anal. Calorim.* 147 (2022) 4597–4610, <https://doi.org/10.1007/s10973-021-10864-6>.
- [33] C.-X. Zhao, Y. Liu, D.-Y. Wang, D.-L. Wang, Y.-Z. Wang, Synergistic effect of ammonium polyphosphate and layered double hydroxide on flame retardant properties of poly(vinyl alcohol), *Polym. Degrad. Stab.* 93 (2008) 1323–1331, <https://doi.org/10.1016/j.polymdegradstab.2008.04.002>.
- [34] J. Wei, C. Zhao, Z. Hou, Y. Li, H. Li, D. Xiang, Y. Wu, Y. Que, Preparation, properties, and mechanism of flame-retardant Poly(vinyl alcohol) aerogels based on the multi-directional freezing method, *Int. J. Mol. Sci.* 23 (2022) 15919, <https://doi.org/10.3390/ijms232415919>.
- [35] W. Yang, S. Qiu, Y. Zhou, B. Zou, J. Wang, P. Jia, L. Song, Nanolayered Graphene/Black phosphorus films for fire-retardant coatings, *ACS Appl. Nano Mater.* 5 (2022) 14841–14849, <https://doi.org/10.1021/acsnano.2c03134>.
- [36] M. Farrokhi, M. Abdollahi, A. Alizadeh, An efficient method for straightforward phosphorylation of ethylene/vinyl alcohol copolymers using trialkyl phosphite/iodine, *Polymer* 169 (2019) 215–224, <https://doi.org/10.1016/j.polymer.2019.02.050>.
- [37] L. Liu, Y. Liu, Y. Liu, Q. Wang, Efficient flame retardant polyvinyl alcohol membrane through surface graft method, *RSC Adv.* 6 (2016) 35051–35057, <https://doi.org/10.1039/C5RA27105C>.
- [38] S. Scurti, E. Monti, E. Rodríguez-Aguado, D. Caretti, J.A. Cecilia, N. Dimitratos, Effect of polyvinyl alcohol ligands on supported gold nano-catalysts: morphological and kinetics studies, *Nanomaterials* 11 (2021) 879, <https://doi.org/10.3390/nano11040879>.
- [39] Y. An, T. Ushida, M. Susuki, T. Koyama, K. Hanabusa, H. Shirai, Complex formation of partially phosphorylated poly(vinyl alcohol), with metal ions in aqueous solution, *Polymer* 37 (1996) 3097–3100, [https://doi.org/10.1016/0032-3861\(96\)89410-9](https://doi.org/10.1016/0032-3861(96)89410-9).
- [40] M. Venkatesh, P. Ravi, S.P. Tewari, Isoconversional kinetic analysis of decomposition of nitroimidazoles: friedman method vs Flynn–Wall–Ozawa method, *J. Phys. Chem. A* 117 (2013) 10162–10169, <https://doi.org/10.1021/jp407526r>.
- [41] H.L. Friedman, Kinetics of thermal degradation of char-forming plastics from thermogravimetry. Application to a phenolic plastic, *J. Polym. Sci. Part C Polym. Symp.* 6 (1964) 183–195, <https://doi.org/10.1002/polc.5070060121>.
- [42] A.W. Coats, J.P. Redfern, Kinetic parameters from thermogravimetric data, *Nature* 201 (1964) 68–69, <https://doi.org/10.1038/201068a0>.
- [43] S. Habibu, N.M. Sarih, N.A. Sairi, M. Zulkifli, Rheological and thermal degradation properties of hyperbranched polyisoprene prepared by anionic polymerization, *R. Soc. Open Sci.* 6 (2019), 190869, <https://doi.org/10.1098/rsos.190869>.
- [44] K. Chrissafis, in: *Kinetics of Thermal Degradation of Polymers Complementary Use of Isoconversional and Model-fitting Methods*, 2009, p. 11.
- [45] C.D. Doyle, Kinetic analysis of thermogravimetric data, *J. Appl. Polym. Sci.* 5 (1961) 285–292, <https://doi.org/10.1002/app.1961.070051506>.

- [46] J.H. Flynn, Energy of Activation, Preexponential Factor and Order of Reaction (When Applicable), (n.d.) 13.
- [47] T. Ozawa, A new method of analyzing thermogravimetric data, *Bull. Chem. Soc. Jpn.* 38 (1965) 1881–1886, <https://doi.org/10.1246/bcsj.38.1881>.
- [48] W. Xie, Z. Han, Z. Zhang, Y. Liu, Q. Wang, Hydrogen bond complexation to prepare guanidine phosphate flame retardant poly(vinyl alcohol) membrane with high transparency, *Compos. Part B Eng.* 176 (2019), 107265, <https://doi.org/10.1016/j.compositesb.2019.107265>.
- [49] Y. Lin, J. Chen, H. Li, Outstanding flame retardancy for poly(vinyl alcohol) achieved using a resveratrol/tannic acid complex, *RSC Adv.* 12 (2022) 285–296, <https://doi.org/10.1039/D1RA08000H>.
- [50] S. Peng, M. Zhou, F. Liu, C. Zhang, X. Liu, J. Liu, L. Zou, J. Chen, Flame-retardant polyvinyl alcohol membrane with high transparency based on a reactive phosphorus-containing compound, *R. Soc. Open Sci.* 4 (2017), 170512, <https://doi.org/10.1098/rsos.170512>.
- [51] M. Banks, J.R. Ebdon, M. Johnson, Influence of covalently bound phosphorus-containing groups on the flammability of poly(vinyl alcohol), poly(ethylene-co-vinyl alcohol) and low-density polyethylene, *Polymer* 34 (1993) 4547–4556, [https://doi.org/10.1016/0032-3861\(93\)90163-5](https://doi.org/10.1016/0032-3861(93)90163-5).
- [52] B. Cademenun, Characterizing phosphorus in environmental and agricultural samples by <sup>31</sup>P nuclear magnetic resonance spectroscopy, *Talanta* 66 (2005) 359–371, <https://doi.org/10.1016/j.talanta.2004.12.024>.
- [53] A. Mohamed Saat, M.R. Johan, The surface structure and thermal properties of novel polymer composite films based on partially phosphorylated Poly(vinyl alcohol) with aluminum phosphate, *Sci. World J.* 2014 (2014) 1–7, <https://doi.org/10.1155/2014/439839>.
- [54] J. Shen, P. Zhang, L. Song, J. Li, B. Ji, J. Li, L. Chen, Polyethylene glycol supported by phosphorylated polyvinyl alcohol/graphene aerogel as a high thermal stability phase change material, *Compos. Part B Eng.* 179 (2019), 107545, <https://doi.org/10.1016/j.compositesb.2019.107545>.
- [55] J. Dai, Y. Peng, N. Teng, Y. Liu, C. Liu, X. Shen, S. Mahmud, J. Zhu, X. Liu, High-performing and fire-resistant biobased epoxy resin from renewable sources, *ACS Sustain. Chem. Eng.* 6 (2018) 7589–7599, <https://doi.org/10.1021/acssuschemeng.8b00439>.
- [56] A. Cingolani, V. Zanotti, C. Cesari, M. Ferri, L. Mazzocchetti, T. Benelli, S. Merighi, L. Giorgini, R. Mazzoni, Synthesis of functionalized iron N-heterocyclic carbene complexes and their potential application as flame behavior modifier in cross linked epoxy resins, *Inorg. Chim. Acta.* 519 (2021), 120273, <https://doi.org/10.1016/j.ica.2021.120273>.
- [57] J.R. Opfermann, E. Kaisersberger, H.J. Flammersheim, Model-free analysis of thermoanalytical data—advantages and limitations, *Thermochim. Acta* 391 (2002) 119–127, [https://doi.org/10.1016/S0040-6031\(02\)00169-7](https://doi.org/10.1016/S0040-6031(02)00169-7).
- [58] S. Bano, N. Ramzan, T. Iqbal, H. Mahmood, F. Saeed, Study of thermal degradation behavior and kinetics of ABS/PC blend, *Pol. J. Chem. Technol.* 22 (2020) 64–69, <https://doi.org/10.2478/pjct-2020-0029>.
- [59] F. Ravari, M. Noori, M. Ehsani, Thermal stability and degradation kinetic studies of PVA/RGO using the model-fitting and isoconversional (model-free) methods, *Fibers Polym.* 20 (2019) 472–480, <https://doi.org/10.1007/s12221-019-8606-8>.
- [60] B. Scharrel, T.R. Hull, Development of fire-retarded materials—Interpretation of cone calorimeter data, *Fire Mater.* 31 (2007) 327–354, <https://doi.org/10.1002/fam.949>.
- [61] L. Mazzocchetti, T. Benelli, G. Zattini, E. Maccaferri, G. Brancolini, L. Giorgini, Evaluation of carbon fibers structure and morphology after their recycling via pyro-gassification of CFRPs, in: *Ischia, Italy, 2019*: p. p. 020036, <https://doi.org/10.1063/1.5140309>.